Catalysis Today 147S (2009) S66–S70

Contents lists available at ScienceDirect

Catalysis Today

journal homepage: www.elsevier.com/locate/cattod

Preparation of nickel phosphide/SBA-15/cordierite monolithic catalysts and catalytic activity for hydrodesulfurization of dibenzothiophene

Ni Wei, Shengfu Ji *, Pingyi Wu, Yanan Guo, Hui Liu, Jiqing Zhu, Chengyue Li

State Key Laboratory of Chemical Resource Engineering, Beijing University of Chemical Technology, Beijing 100029, China

ARTICLE INFO

Article history:
Available online 5 August 2009

Keywords:
Nickel phosphides
SBA-15
Cordierite
Monolithic catalysts
Hydrodesulfurization
Dibenzothiophene

ABSTRACT

A series of nickel phosphide/SBA-15/cordierite monolithic catalysts with Ni contents from 2.5 wt.% to 12.4 wt.% and initial P/Ni molar ratio of 1/2 were prepared and their activity for the hydrodesufurization (HDS) of dibenzothiophene (DBT) was evaluated. The structure of the catalysts was investigated by X-ray diffraction (XRD), N_2 adsorption–desorption isotherms and scanning electron microscope (SEM). The results showed that the nickel phosphides phase had not been observed in the monolithic catalysts when Ni content was less than 7.4 wt.%. The Ni_2P phase and $Ni_{12}P_5$ phase were found when Ni content was from 9.9 wt.% to 12.4 wt.%. The DBT conversion can reach 99.2% at 380 °C when Ni content was 9.9 wt.%. The activity of the monolithic catalyst was as good as that for the nickel phosphide/SBA-15 powder catalyst at 380 °C for the HDS of DBT, which indicated that there was no diffusive restriction on monolithic catalysts. Biphenyl (BP) selectivity over the monolithic catalysts was evidently higher than that for the nickel phosphide/SBA-15 powder catalyst when the temperature was over 320 °C.

1. Introduction

Today, severe environmental regulations are enacted to limit the sulfur contents in fuel. It has been recognized that the current commercial hydrodesulfurization (HDS) catalysts are not adequate to meet the regulation requirements [1]. This urges the worldwide research efforts to find new HDS catalysts, in which nickel phosphides are believed to be the next-generation HDS catalysts for their excellent performance in HDS [2–5]. The supported nickel phosphide catalysts usually use SiO_2 as a support [2,3]. The obtained catalysts have a poor dispersion of active components resulting in the low catalytic activity.

Mesoporous molecular sieves have been recognized as the good catalytic supports for their high specific area and pore volume as well as the uniform pore size distribution [6]. Oyama and Lee [7] prepared Ni_2P catalysts supported on SiO_2 and MCM-41 and found that Ni_2P/MCM-41 has the best catalytic activity. Compared with MCM-41, SBA-15 [8] has larger pore diameter and better thermal stability. Korányi et al. [9,10] prepared a series of Ni_2P and $Ni_{12}P_5$ supported on SBA-15 ordered mesoporous silica and investigated their catalytic activities for HDS and HDN. In our previous studies [11], a series of Ni_2P/SBA-15 catalysts with different Ni contents were prepared. The obtained catalysts showed the excellent catalytic activity for the HDS of thiophene and DBT. In recent years, the monolithic catalysts have attracted considerable attention and are widely applied in the environmental field as the support [12–15]. However, the applications of monolith catalysts in HDS are quite few. Edvinsson and Irandoust [16] studied Co–Mo/γ-$A1_2O_3$ supported on monolith for HDS of DBT and found the use of a monolithic catalyst reactor exhibits several attractive features. Almost no scale dependency and low pressure drop were the most important.

In this study, the nickel phosphide/SBA-15/cordierite monolithic catalysts with different Ni contents were prepared using cordierite as support and nickel phosphide/SBA-15 as coating. The catalytic activity for HDS of DBT was tested. The structure was investigated by XRD, N_2 adsorption–desorption isotherms and SEM.

2. Experimental

2.1. Catalyst preparation

SBA-15 was synthesized by using the literature method [17]. Typically, a homogenous mixture composed of Pluronic P123 triblock copolymers (EO_{20}-PO_{70}-EO_{20}) and tetraethyl orthosilicate (TEOS) in hydrochloric acid was stirred at 40 °C for 22 h, and further treated at 100 °C for 24 h. The resultant solid was filtered, washed, dried and finally calcined at 550 °C for 6 h. Nickel phosphate/SBA-15 was prepared by impregnating appropriate

* Corresponding author. Tel.: +86 10 64419619; fax: +86 10 64419619.
E-mail address: jisf@mail.buct.edu.cn (S. Ji).

0920-5861/$ – see front matter © 2009 Elsevier B.V. All rights reserved.
doi:10.1016/j.cattod.2009.07.053

amounts of an aqueous solution of $(NH_4)_2HPO_4$ and Ni $(NO_3)_2{\cdot}6H_2O$ with P/Ni molar ratio of 1/2 to SBA-15, then drying at 120 °C for 24 h and calcining at 550 °C for 4 h. The nickel phosphate/SBA-15 slurry was prepared from nickel phosphate/SBA-15 powder.

Commercial cordierite with a cell density of 300 cpsi was cut to obtain samples with diameter of 9 mm and length of 50 mm. Then, the obtained cordierite samples were pretreated by using 10 wt.% oxalic acid solution boiling for 2 h, washed with deionized water, and finally calcined at 300 °C for 3 h. These monolith supports were dipped into the nickel phosphate/SBA-15 slurry prepared above, dried at room temperature in air, and then calcined at 500 °C for 4 h. This procedure was repeated several times to achieve the desired coating amount. The precursors of monolithic catalysts were obtained. Finally, nickel phosphide/SBA-15/cordierite monolithic catalysts were prepared by temperature programmed reduction (TPR) method in a fixed-bed continuous flow stainless steel reactor at atmospheric pressure in the H_2 flow rate of 100 $cm^3\ min^{-1}$. The temperature was increased from room temperature (RT) to 300 °C at a rate of 10 °C min^{-1}, from 300 °C to 650 °C at a rate of 1 °C min^{-1}, and finally maintained at 650 °C for 2 h. After TPR, the sample was cooled to RT and passivated by 1% O_2/Ar (v/v) for structure characterization, or the reaction feed was introduced for HDS of DBT. The obtained catalysts were denoted as Ni_xP/SBA-15/cordierite. The loading of Ni_xP/SBA-15 was about 20 wt.% of the whole catalyst. The loading of Ni based on whole catalyst was listed in Table 1.

2.2. Catalyst characterization

XRD patterns of cordierite monolithic catalysts were obtained on a Rigaku D/Max 2500 VB2+/PC diffractometer using CuKα radiation operating at 200 mA and 40 kV. N_2 adsorption–desorption isotherms of cordierite monolithic catalysts were measured by using a Thermo Electron Sorptomatic 1990 instrument. Before each measurement, the sample was outgassed for at least 5 h at 250 °C under vacuum. BET and BJH methods were used to determine the specific surface area and pore size distribution, respectively. The morphology of the samples was observed by a ZEISS SUPRA ™55 field emission scanning electron microscope. The coating adhesion was measured by an ultrasonic method and the weight loss of the washcoat layer was less than 3 wt.%.

2.3. Catalytic activity measurement

The HDS of DBT was performed in a high-pressure fixed-bed continuous flow stainless steel reactor (9 mm in diameter and 500 mm in length) with a central thermocouple to measure the temperature of the catalyst bed. Hydrogen flow was regulated by a mass flow controller. The reaction temperature was from 300 °C to 380 °C, a liquid hourly space velocity (LHSV) was 1.9 h^{-1}, a ratio of hydrogen to liquid feed was 400 (v/v), and reaction pressure was 3.0 MPa. The reaction feed consisting of 1 wt.% DBT in decalin was introduced into the reactor by a piston pump. The liquid products were collected at 1 h intervals and analyzed off-line by a gas chromatography (SP2100, Beijing Beifenruili Analytic Instrument (Group) Co., Ltd) equipped with a flame ionization detector (FID) and a capillary column (HJ. PONA, 50 m × 0.20 mm × 0.50 μm). The main products of the reaction were biphenyl (BP) and cyclohexylbenzene (CHB). Therefore, the conversion of DBT can be used to measure the HDS performance of the monolithic catalysts.

Table 1
Physico-chemical properties of cordierite and Ni_xP/SBA-15/cordierite samples.

Sample	Ni (wt.%)	S_{BET} ($m^2\ g^{-1}$)	V_P ($cm^3\ g^{-1}$)	D_{BJH} (nm)
Pretreated cordierite	–	17	0.02	3.6
Ni_xP/SBA-15/cordierite-1	2.5	131	0.21	6.2
Ni_xP/SBA-15/cordierite-2	4.9	142	0.22	5.6
Ni_xP/SBA-15/cordierite-3	7.4	159	0.26	3.8
Ni_xP/SBA-15/cordierite-4	9.9	185	0.27	4.2
Ni_xP/SBA-15/cordierite-5	12.4	154	0.26	4.0

3. Results and discussion

3.1. XRD

XRD patterns of cordierite and Ni_xP/SBA-15/cordierite samples are shown in Fig. 1. As seen in the figure, cordierite had its own characteristic diffraction peaks at 18.0°, 19.0°, 21.6°, 26.4°, 28.4°, 29.4°, 33.8°, 36.8°, 38.4°, 42.9° and 54.2°, corresponding to the structure of ceramic [18]. For the acid-pretreated cordierite, the intensity of these peaks decreased. For all Ni_xP/SBA-15/cordierite

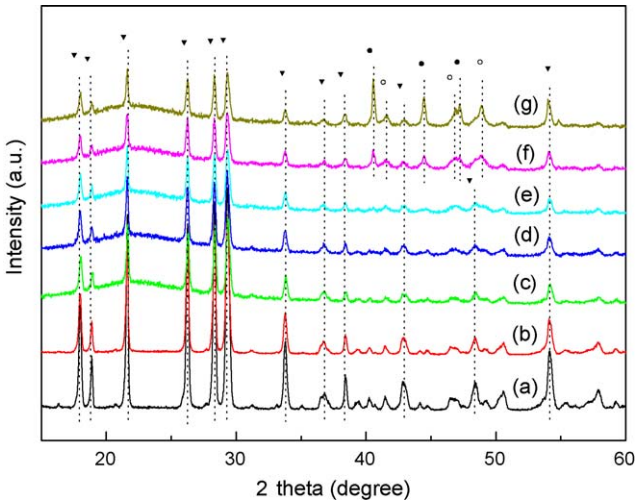

Fig. 1. XRD patterns of cordierite and Ni_xP/SBA-15/cordierite samples: (a) cordierite; (b) pretreated cordierite; (c) Ni_xP/SBA-15/cordierite-1; (d) Ni_xP/SBA-15/cordierite-2; (e) Ni_xP/SBA-15/cordierite-3; (f) Ni_xP/SBA-15/cordierite-4; (g) Ni_xP/SBA-15/cordierite-5 (symbols: ▼, cordierite; ○, $Ni_{12}P_5$; ●, Ni_2P).

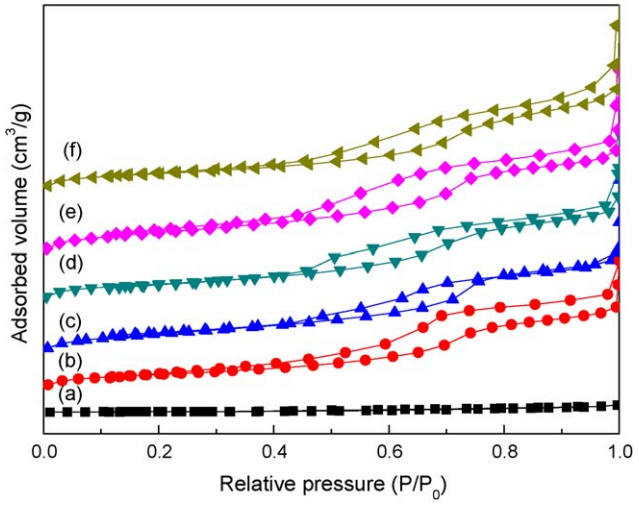

Fig. 2. N_2 adsorption–desorption isotherms of cordierite and Ni_xP/SBA-15/cordierite samples: (a) pretreated cordierite; (b) Ni_xP/SBA-15/cordierite-1; (c) Ni_xP/SBA-15/cordierite-2; (d) Ni_xP/SBA-15/cordierite-3; (e) Ni_xP/SBA-15/cordierite-4; (f) Ni_xP/SBA-15/cordierite-5.

samples, the main diffraction peaks of cordierite were retained, but the intensity of these peaks gradually decreased with the increase of Ni contents. For Ni_xP/SBA-15/cordierite-1, Ni_xP/SBA-15/cordierite-2 and Ni_xP/SBA-15/cordierite-3, no diffraction peaks of nickel phosphide phases were found, indicating that the nickel phosphide phases were well dispersed on the surface of catalyst. For Ni_xP/SBA-15/cordierite-4, it can be seen that besides the diffraction peaks of cordierite, some new diffraction peaks should be easily identified, in which the peaks at 41.6°, 46.8° and 48.8° can be assigned to $Ni_{12}P_5$, and the peaks at 40.6°, 44.5° and 47.2° can be assigned to Ni_2P [2,9,10], demonstrating the appearance of Ni_2P and $Ni_{12}P_5$ crystallites. The intensity of these diffraction peaks ascribed to nickel phosphides increased in Ni_xP/SBA-15/cordierite-5. It indicated that the active phases of Ni_xP/SBA-15/cordierite-4 and Ni_xP/SBA-15/cordierite-5 were Ni_2P and $Ni_{12}P_5$. This may be due to the initial P/Ni molar ratio (1/2) employed in our experiments. Oyama et al. [2] studied the effect of phosphorus content on the structure and activity of Ni_2P/SiO_2, and found that at the initial P/Ni molar ratio of 1/2 (stoichiometric ratio of Ni_2P), the sample contained two phases (Ni_2P and $Ni_{12}P_5$). Korányi et al. [9]

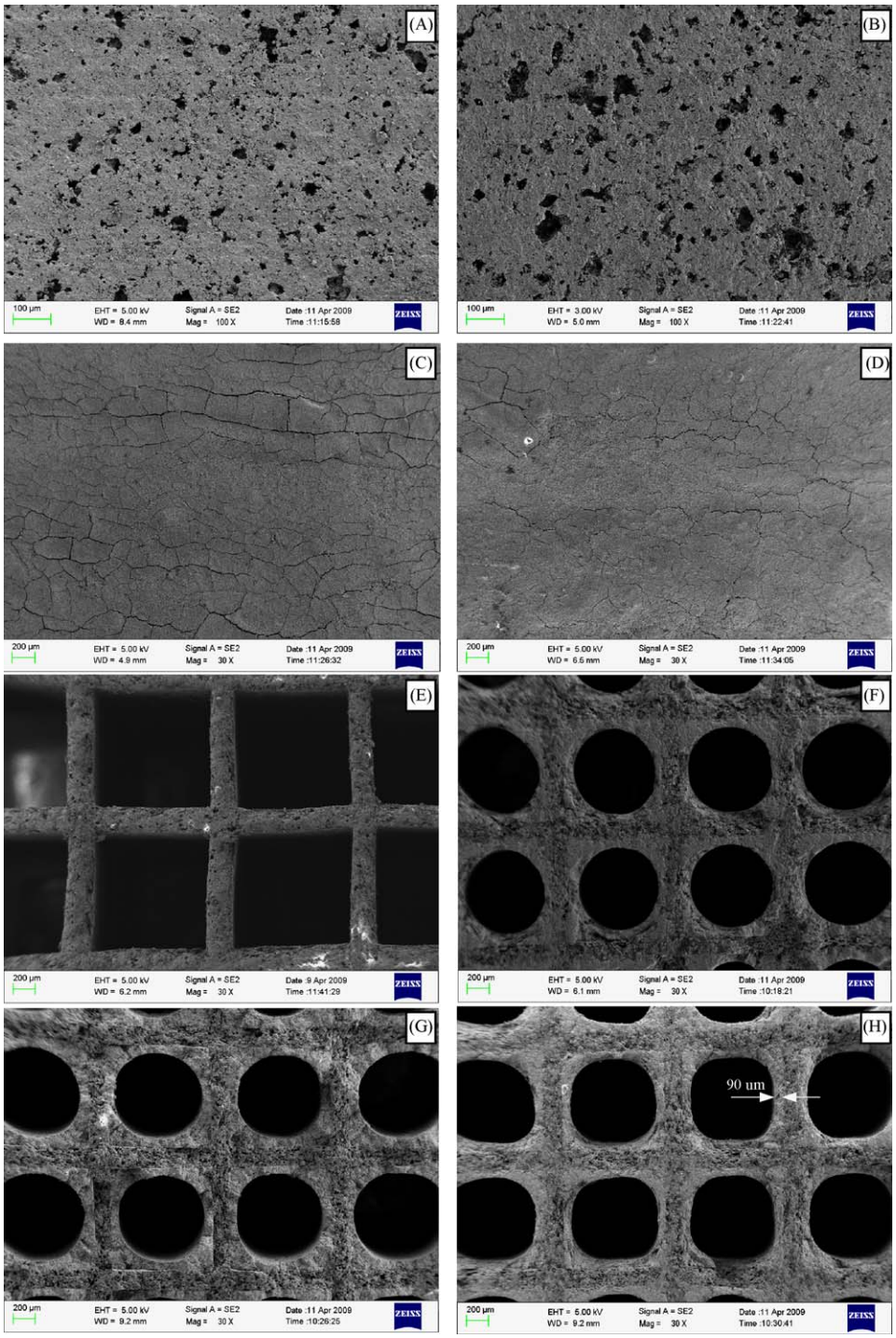

Fig. 3. SEM images of cordierite and Ni_xP/SBA-15/cordierite samples: (a) cordierite (surface); (b) pretreated cordierite (surface); (c) Ni_xP/SBA-15/cordierite-2 (surface); (d) Ni_xP/SBA-15/cordierite-5 (surface); (e) pretreated cordierite (cross section); (f) Ni_xP/SBA-15/cordierite-2 (cross section); (g) Ni_xP/SBA-15/cordierite-4 (cross section); (h) Ni_xP/SBA-15/cordierite-5 (cross section).

also reported that a mixture of Ni_2P and $Ni_{12}P_5$ was found in the SBA-15 and CMK-5 supported nickel phosphide catalysts with initial molar ratio of P/Ni = 1/2, respectively. Suggesting that in the monolithic catalysts, the nickel phosphide phases were the Ni_2P and $Ni_{12}P_5$.

3.2. N_2 adsorption–desorption isotherms

N_2 adsorption–desorption isotherms of cordierite and Ni_xP/SBA-15/cordierite samples are shown in Fig. 2. Table 1 summarizes the physico-chemical properties of samples. It can be seen from Fig. 1 that the nitrogen adsorption–desorption isotherms of pretreated cordierite had a very small hysteresis loop, while the isotherms of all Ni_xP/SBA-15/cordierite catalysts were found to be of type IV according to the IUPAC classification and exhibited a H1 hysteresis loop that is typical of mesoporous solid [19]. The cordierite without acid pretreatment has very low specific surface area ($<1\ m^2\ g^{-1}$) and has few mesopores or micropores. After pretreatment, the S_{BET} and V_p of cordierite increased to $17\ m^2\ g^{-1}$ and $0.02\ cm^3\ g^{-1}$, respectively. It also had a mesopore with D_{BJH} of 3.4 nm. Compared with the pretreated cordierite, the pore parameters (S_{BET}, V_p and D_{BJH}) of all Ni_xP/SBA-15/cordierite catalysts increased significantly, in which Ni_xP/SBA-15/cordierite-4 had the highest values of S_{BET} ($185\ m^2\ g^{-1}$) and V_p ($0.27\ cm^3\ g^{-1}$). It indicated that the specific surface area and pore volume of monolithic catalysts were mainly supplied by Ni_xP/SBA-15 coating in the Ni_xP/SBA-15/cordierite catalysts.

3.3. SEM

Fig. 3 shows the SEM images of cordierite and Ni_xP/SBA-15/cordierite samples. From the surface view of cordierite (Fig. 3(a) and (b)), it can be seen that after acid pretreatment, the surface of cordierite became more coarse and had more macropores. This benefited the coating of Ni_xP/SBA-15. Fig. 3(c) and (d) show that the coating layer is homogeneously deposited on the cordierite support. Some small cracks can be observed in these two images. This may be due to the calcination process. From the cross sectional view of cordierite (Fig. 3 (e)), the wall thickness of cordierite was about 230 μm. Fig. 3(f), (g) and (h) revealed that Ni_xP/SBA-15/cordierite samples obtained round channels. The thickness of coating layer of all Ni_xP/SBA-15/cordierite catalysts was similar and it was about 90 μm (Fig. 3(h)).

3.4. Catalytic activity

Fig. 4 presents the activity of Ni_xP/SBA-15/cordierite monolithic catalysts and the Ni_xP/SBA-15 powder catalyst for HDS of DBT. The impregnation procedure for Ni_xP/SBA-15 powder catalyst is described elsewhere [11]. As observed, the DBT conversion increased with increasing temperature and nickel content for all monolithic catalysts. The DBT conversion over the Ni_xP/SBA-15/cordierite-4 catalyst was 99.2% at 380 °C. The Ni_xP/SBA-15/cordierite-4 catalyst and the Ni_xP/SBA-15 powder catalyst had the same Ni content based on SBA-15 and initial P/Ni ratio. Below 380 °C, it was observed that the activity of the Ni_xP/SBA-15/cordierite-4 catalyst was lower than that for the Ni_xP/SBA-15 powder catalyst under the same condition of the weight hourly space velocity (WHSV). It indicated that there were diffusive restrictions on the Ni_xP/SBA-15/cordierite-4 catalyst. However, the activity of the Ni_xP/SBA-15/cordierite-4 catalyst was as good as that for the Ni_xP/SBA-15 powder catalyst at 380 °C, which indicated that there were no diffusive restrictions on Ni_xP/SBA-15/cordierite-4 catalyst. Fig. 5 shows the BP and CHB selectivity over Ni_xP/SBA-15/cordierite monolithic catalysts and the Ni_xP/SBA-15 powder catalyst for HDS of DBT. It can be seen that the BP

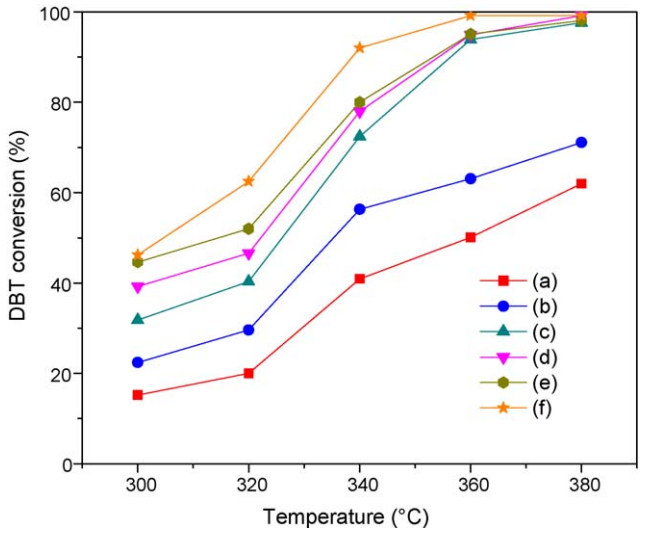

Fig. 4. Catalytic activity of Ni_xP/SBA-15/cordierite monolithic catalysts for HDS of DBT: (a) Ni_xP/SBA-15/cordierite-1; (b) Ni_xP/SBA-15/cordierite-2; (c) Ni_xP/SBA-15/cordierite-3; (d) Ni_xP/SBA-15/cordierite-4; (e) Ni_xP/SBA-15/cordierite-5;(f) Ni_xP/SBA-15 powder.

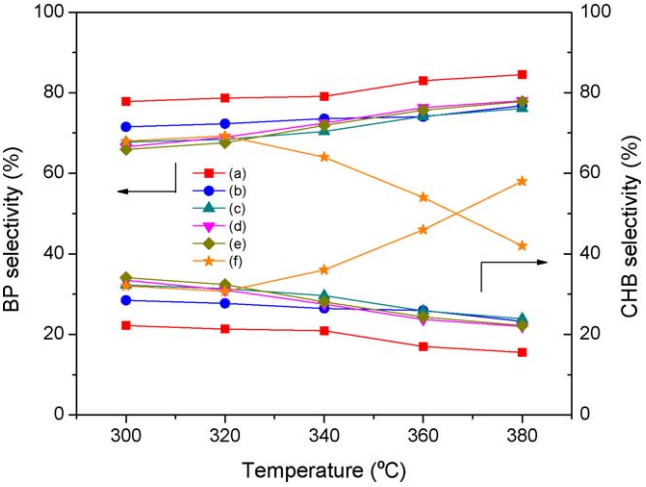

Fig. 5. BP and CHB selectivity over Ni_xP/SBA-15/cordierite monolithic catalysts for HDS of DBT: (a) Ni_xP/SBA-15/cordierite-1; (b) Ni_xP/SBA-15/cordierite-2; (c) Ni_xP/SBA-15/cordierite-3; (d) Ni_xP/SBA-15/cordierite-4; (e) Ni_xP/SBA-15/cordierite-5; (f) Ni_xP/SBA-15 powder.

selectivity over all monolithic catalysts was higher than that for Ni_xP/SBA-15 powder catalyst when the temperature was over 320 °C. It indicated that the monolithic catalysts might improve the selectivity of product. The result was similar with the result of the study of the Nijhuis et al. [20].

Fig. 6 gives the mechanism of the HDS of DBT on Ni_xP/SBA-15/cordierite monolithic catalysts. The HDS of DBT reaction products

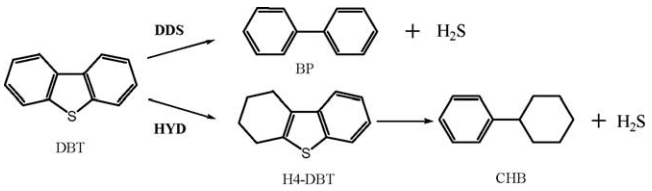

Fig. 6. Mechanism of the HDS of DBT on Ni_xP/SBA-15/cordierite monolithic catalysts.

are BP, CHB and traces of H4-DBT (can be neglected). The conversion of DBT can occur through two parallel reactions, direct desulfurization (DDS) and desulfurization after hydrogenation (HYD). For DDS route, the main product is BP. For HYD route, H4-DBT is first yielded and then quickly converted to CHB. For Ni_xP/SBA-15/cordierite monolithic catalysts, it is obvious that BP produced by the DDS route is the main product with the selectivity higher than 65%. It indicated that the HDS of DBT was mainly the DDS route in the nickel phosphide/SBA-15/cordierite monolithic catalysts.

4. Conclusion

A series of Ni_xP/SBA-15/cordierite monolithic catalysts with different Ni contents and initial P/Ni molar ratio of 1/2 were prepared. For the Ni_xP/SBA-15/cordierite-1, Ni_xP/SBA-15/cordierite-2 and Ni_xP/SBA-15/cordierite-3 catalysts, the nickel phosphides were well dispersed on the monolithic catalysts. For the Ni_xP/SBA-15/cordierite-4 and Ni_xP/SBA-15/cordierite-5 catalysts, the nickel phosphide phase was Ni_2P and $Ni_{12}P_5$. The coating of Ni_xP/SBA-15 on cordierite support can significantly increase the specific surface area and pore volume, in which the Ni_xP/SBA-15/cordierite-4 catalyst had the highest values of S_{BET} ($185\ m^2\ g^{-1}$) and V_p ($0.27\ cm^3\ g^{-1}$). The activity of the Ni_xP/SBA-15/cordierite-4 catalyst was as good as the Ni_xP/SBA-15 powder catalyst at 380 °C. The BP selectivity over all monolithic catalysts was higher than that for Ni_xP/SBA-15 powder catalyst when the temperature was over 320 °C. For all Ni_xP/SBA-15/cordierite monolithic catalysts, the reaction route for HDS of DBT over nickel phosphide/SBA-15/cordierite monolithic catalysts is mainly DDS.

Acknowledgements

The authors thank for the financial support of the National Natural Science Foundation of China (Grant 20473009) and the National Basic Research Program of China (973 Project No. 2006CB202503).

References

[1] C. Song, Catal. Today 86 (2003) 211.
[2] S.T. Oyama, X. Wang, Y.-K. Lee, K. Bando, F.G. Requejo, J. Catal. 210 (2002) 217.
[3] S.T. Oyama, X. Wang, F. Requejo, T. Sato, Y. Yoshimura, J. Catal. 209 (2002) 1.
[4] S.T. Oyama, J. Catal. 216 (2003) 343.
[5] S.F. Song, C.H. Liang, R. Prins, J. Catal. 237 (2006) 118.
[6] J.S. Beck, J.C. Vartuli, W.J. Roth, M.E. Leonowicz, C.T. Kresge, K.D. Schmitt, C.T.-W. Chu, D.H. Olson, E.W. Sheppard, S.B. McCullen, J.B. Higgins, J.L. Schlenker, J. Am. Chem. Soc. 114 (1992) 10834.
[7] S.T. Oyama, Y.K. Lee, J. Catal. 258 (2008) 393.
[8] D. Zhao, J. Feng, Q. Huo, N. Melosh, G.H. Fredrickson, B.F. Chmelka, G.D. Stucky, Science 279 (1998) 548.
[9] T.I. Korányi, Z. Vít, J.B. Nagy, Catal. Today 130 (2008) 80.
[10] T.I. Korányi, Z. Vít, D.G. Poduval, R. Ryoo, H.S. Kim, E.J.M. Hensen, J. Catal. 253 (2008) 119.
[11] X. Huang, S. Ji, P. Wu, Q. Liu, H. Liu, J. Zhu, C. Li, Acta Phys.: Chim. Sin. 24 (2008) 1773.
[12] P. Avila, M. Montes, E.E. Miró, J. Chem. Eng. 109 (2005) 11.
[13] J.M. Zamaro, M.A. Ulla, E.E. Miró, Chem. Eng. J. 106 (2005) 25.
[14] R.D. Clayton, M.P. Harold, V. Balakotaiah, Appl. Catal. B: Environ. 84 (2008) 616.
[15] B.P. Barbero, L. Costa-Almeida, O. Sanz, Chem. Eng. J. 139 (2008) 430.
[16] R. Edvinsson, S. Irandoust, Ind. Eng. Chem. Res. 32 (1993) 391.
[17] D. Zhao, J. Sun, Q. Li, G.D. Stucky, Chem. Mater. 12 (2000) 275.
[18] L. Li, B. Xue, J. Chen, N. Guan, F. Zhang, D. Liu, H. Feng, Appl. Catal. A: Gen. 292 (2005) 312.
[19] M. Kruk, M. Jaroniec, Chem. Mater. 13 (2001) 3169.
[20] T.A. Nijhuis, M.T. Kreutzer, A.C.J. Romijn, F. Kapteijn, J.A. Moulijn, Chem. Eng. Sci. 56 (2001) 823.